The European Research Journal 2026;12(4):447-456 Original Article

DOI: https://doi.org/10.18621/eurj.1669895 *Radiology*

Could Ratio-Based Morphometric Analysis of Subcortical Limbic Structures Assist in Alzheimer's Disease Diagnosis?

Meryem Esma Düz[1], Muzaffer Şeker[2], Nurullah Yücel[3], Cengiz Erol[4], Lütfü Hanoğlu[5], Gülhan Ertan Akan[6]

[1]Department of Anatomy, School of Medicine, Ankara Medipol University, Ankara, Türkiye; [2]Turkish Academy of Sciences, Ankara, Türkiye; [3]Department of Anatomy, Hamidiye School of Medicine, University of Health Sciences, İstanbul, Türkiye; [4]Department of Radiology, School of Medicine, İstanbul Medipol University, İstanbul, Türkiye; [5]Department of Neurology, School of Medicine, Istanbul Medipol University, İstanbul, Türkiye; [6]Department of Radiology, School of Medicine, Istanbul Medipol University, İstanbul, Türkiye

ABSTRACT

Objectives: Alzheimer's disease is a neurodegenerative disorder that primarily affects subcortical limbic structures. This study aimed to assess volumetric differences in subcortical limbic structures and to compare the relative volumes of surrounding brain regions - such as the telencephalon, diencephalon, and brainstem subdivisions - between individuals with Alzheimer's disease and healthy controls.

Methods: This study involved 24 patients with Alzheimer's disease and 16 healthy controls. Subcortical structures were segmented automatically using MRICloud on 3D T1-weighted magnetic resonance imaging scans. To minimize individual anatomical variability, volume ratios relative to neighboring brain regions were also calculated.

Results: Significant volume reductions were found in the amygdala (left: P=0.004, right: P=0.005, total: P=0.004), hypothalamus (left: P=0.005, right: P>0.05, total: P=0.007), diencephalon (left: P=0.001, right: P=0.012, total: P>0.05), and mammillary bodies (left: P=0.002, right: P=0.003, total: P=0.003) in the Alzheimer's disease group compared to healthy controls. Although most volume ratios - particularly those involving the amygdala and mammillary bodies - were higher in the Alzheimer's disease group, they did not reach statistical significance (P>0.05).

Conclusions: This study confirms prominent atrophy in subcortical limbic structures in Alzheimer's disease. While diencephalon volume was reduced, its ratio to the amygdalae changed minimally, likely reflecting more severe atrophy of the amygdalae. Similarly, the mesencephalon-to-hypothalamus ratio showed no significant difference, suggesting parallel atrophy. These findings support the combined use of absolute and ratio-based analyses and demonstrate the potential of MRICloud to identify Alzheimer's disease-related neuroanatomical changes.

Keywords: Alzheimer's Disease, Amygdala, Hypothalamus, Mammillary Bodies, Subcortical Structures, Magnetic Resonance Imaging

Submitted: April 5, 2025 **Accepted:** June 15, 202 **Published Online:** June 29, 2025

How to cite this article: Düz ME, Şeker M, Yücel N, Erol C, Hanoğlu L, Ertan Akan G. Could Ratio-Based Morphometric Analysis of Subcortical Limbic Structures Assist in Alzheimer's Disease Diagnosis? *Eur Res J.* 2026;12(4):447-456. doi: 10.18621/eurj.1669895

Corresponding author: Meryem Esma Düz, MD., Phone: +90 444 20 10, E-mail: esma.duz@ankaramedipol.edu.tr

This is an **open-access** article distributed under the terms of a Creative Commons Attribution-NonCommercial-NoDerivatives 4.0 International License, which permits any non-commercial use, sharing, distribution and reproduction in any medium or format, as long as you give appropriate credit to the original author(s) and the source, provide a link to the Creative Commons licence, and indicate if you modified the licensed material. You do not have permission under this licence to share adapted material derived from this article or parts of it.

Available Online at https://www.eurj.org.tr

Alzheimer's disease (AD) is a progressive and irreversible neurodegenerative disorder that primarily affects older adults, including both elderly individuals and those with early-onset forms. It is characterized by cognitive decline, memory impairment, and behavioral disturbances, and its prevalence is increasing as the global population ages [1, 2]. The number of individuals affected is projected to reach 13.8 million by 2060 [3]. Therefore, accurate and reliable risk prediction is critical for the development of disease-modifying therapies aimed at mitigating the devastating impact of AD.

Several studies based on magnetic resonance imaging (MRI) have demonstrated volume reductions in cortical structures, such as the hippocampus, in individuals with Alzheimer's disease [4]. However, subcortical limbic system structures - including the mammillary bodies, amygdala, thalamus, and hypothalamus - have been less extensively studied. Motor symptoms, which reflect pathological changes in the extrapyramidal system, tend to emerge in the later stages of Alzheimer's disease [5]. Therefore, it is commonly assumed that degeneration in the hippocampus and cortex precedes that in frontal–subcortical circuits [6]. Nevertheless, this widely accepted sequence of degeneration may not fully reflect the underlying pathophysiology. It is often overlooked that other regions of the Papez circuit are affected concurrently with the hippocampus [7], and that the hippocampus constitutes only one component of this interconnected system [8]. Given the possibility that pathological changes in subcortical structures may begin earlier than those in the hippocampus and progressively worsen, volumetric analyses of the amygdala, hypothalamus, and mammillary bodies - structures that have received comparatively less attention in the literature - may offer valuable insights as potential biomarkers for the prediction of AD.

However, relying exclusively on the absolute volumes of these structures may limit diagnostic accuracy due to genetic and structural variability among individuals. For instance, a study by Gerritsen *et al*. [9] demonstrated that, in non-depressed controls, a higher amygdala-to-hippocampus (AH) volume ratio was associated with a stronger bias toward negative memories - a key cognitive marker of depression - whereas weaker associations were observed when the amygdala and hippocampus were assessed separately. Such discrepancies may contribute to suboptimal clinical decision-making or misdiagnosis. Considering the structural and functional interconnectivity of brain regions, evaluating the amygdala, hypothalamus, and mammillary bodies in relation to their adjacent structures may yield more meaningful diagnostic insights than assessing each region independently.

To address these limitations, recent developments in neuroimaging have led to the emergence of automated tools that can analyze both absolute and relative brain volumes. In parallel, web-based platforms for evaluating neuroanatomical structures have gained traction and increasingly supplanted traditional manual measurement methods. MRICloud is one such platform that performs automated volumetric analysis of T1-weighted MRI data and generates comprehensive neuroanatomical profiles. It is suitable for multicenter clinical validation studies, and its reliability in predicting future cognitive decline has been previously validated [10]. Although several studies have used automatic segmentation tools such as volBrain, Computational Anatomy Toolbox (CAT), BrainSuite, and FreeSurfer to evaluate the volumes of the amygdala, hypothalamus, and mammillary bodies in AD, to the best of our knowledge, no study has assessed both the volumes and volume ratios of these structures using the web-based MRICloud platform in AD.

In this study, we analyzed the volumes of the left amygdala (AmygL), right amygdala (AmygR), total amygdala (TotAmyg), left hypothalamus (HypoThL), right hypothalamus (HypoThR), total hypothalamus (TotHypoTh), left mammillary body (MamL), right mammillary body (MamR), and total mammillary body (TotMam). Additionally, we evaluated the volume ratios of surrounding brain regions - including the right and left telencephalon (TelenR and TelenL), total telencephalon (TotTelen), left and right diencephalon (DiencL and DiencR), total diencephalon (TotDienc), and brainstem components such as the mesencephalon (Mesenc), metencephalon (Metenc), and myelencephalon (Myelenc) - relative to these limbic structures using MRICloud. We aimed to explore their potential utility as volumetric biomarkers to enhance diagnostic accuracy in AD.

METHODS

Ethics Approval

This study was approved by the Non-Interventional Clinical Research Ethics Committee of Istanbul Medipol University (February 19, 2020; No: 170).

Study Design

Patients over the age of 50 who presented with complaints of amnesia to the Neurology Outpatient Clinic of Istanbul Medipol University Hospital between January 1, 2017, and December 31, 2019, were retrospectively evaluated. All patients had completed at least primary school education and were diagnosed with AD according to the Diagnostic and Statistical Manual of Mental Disorders, Fifth Edition (DSM-5) criteria. Mini-Mental State Examination (MMSE) scores and T1-weighted MRI scans were retrieved from electronic medical records.

Participants

This study included 24 patients diagnosed with AD and 16 healthy controls (HC), selected from the Neurology Outpatient Clinic of Istanbul Medipol University Hospital between January 2017 and December 2019. All participants met the diagnostic criteria outlined in the DSM-5. The demographic characteristics of the participants are presented in Table 1.

Inclusion and Exclusion Criteria

Participants included individuals aged 55–84 years who underwent 3T MRI and were diagnosed with AD or classified as HC. The AD and HC groups had comparable age and sex distributions. Exclusion criteria included age below 50, illiteracy, space-occupying brain lesions, global brain atrophy, cerebrovascular disease, and other neurodegenerative or structural brain disorders such as Parkinson's disease, amyotrophic lateral sclerosis, essential tremor, and primary or metastatic brain tumors. From the initial sample, 65 patients without 3D T1-weighted MRI images, 33 with mismatched MMSE and MRI dates, 20 with inconsistencies between MMSE scores and clinical findings, and 19 who met other exclusion criteria were excluded. Ultimately, 24 patients with AD (10 males, 14 females) were included in the study. The final sample also included 16 healthy controls (7 males and 9 females).

Structural MRI Protocol

MRI was performed using a 3-T Philips Achieva TX scanner (Philips Healthcare, Best, Netherlands) equipped with a 20-channel head coil. The imaging protocol consisted of 3D T1-weighted and FLAIR sequences. Sagittal T1-weighted images were used for volumetric analysis. Imaging parameters for the T1-weighted Magnetization Prepared Rapid Acquisition Gradient Echo (MPRAGE) sequence were as follows: repetition time (TR) = 2400 ms, echo time (TE) = 3.54 ms, field of view (FOV) = 250 × 250 mm (sagittal plane), slice thickness = 1 mm, voxel size = 1 × 1 × 1 mm, turbo field echo (TFE) factor = 97, flip angle = 8°, and matrix size = 228 × 227 pixels. MRIcron software was used to convert the MRI data into a format suitable for analysis. The preprocessed data were then uploaded to the MRICloud platform.

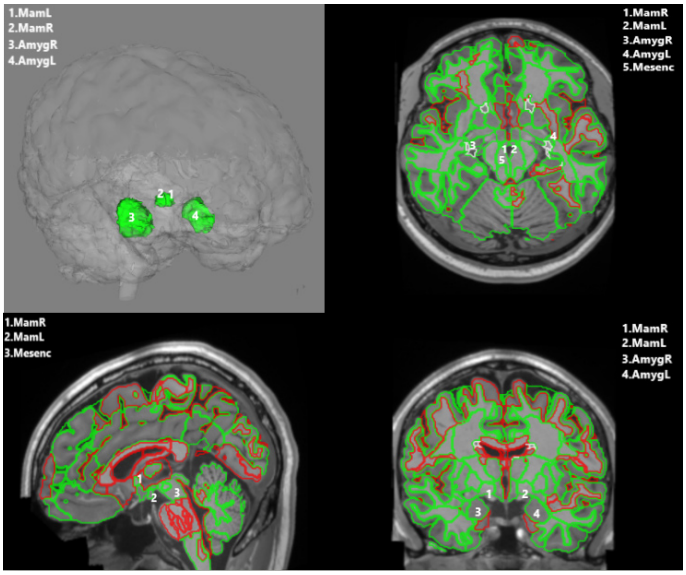


FIGURE 1. Parcellation of MPRAGE images based on the Multi-Atlas Likelihood Fusion algorithm. 3D and cross-sectional views (axial, coronal, and sagittal) illustrate bilateral segmentation of limbic system subcortical structures and mesencephalon: 1. Left Mammillary Body (MamL), 2. Right Mammillary Body (MamR), 3. Right Amygdala (AmygR), 4. Left Amygdala (AmygL), 5. Mesencephalon (Mesenc). Green areas represent the segmented regions overlaid on anatomical MRI sections.

Automatic Segmentation

Magnetic Resonance Imaging Cloud (MRICloud)

MRICloud provides a fully automated segmentation service for MPRAGE images using the Multi-Atlas Likelihood Fusion algorithm, the JHU multi-atlas inventory with 286 labeled structures, and Ontology Level Control [11]. The segmentation atlas used in this study was "adult_286labels_11atlases_V5L" (Figure 1).

DICOM files were converted directly to the Analyze format (.hdr and .img extensions) using the dcm2analyze tool, as recommended by the official MRICloud documentation. This step ensured compatibility with the MRICloud platform, which requires input files in Analyze format. After conversion, the resulting .hdr and .img files were archived and uploaded to MRICloud for automated segmentation and volumetric analysis.

Finally, the archived Analyze format files (.hdr and .img) were uploaded to MRICloud via a web browser. Following the entry of demographic information such as age and gender, volumetric measurement results were made available in the "My Job Status" section as a downloadable .zip file containing the "corrected_stats.txt" table. Segmentation results were visualized in 3D using ITK-SNAP and MRIcroGL, two commonly used neuroimaging tools for anatomical visualization and surface rendering (Figure 2).

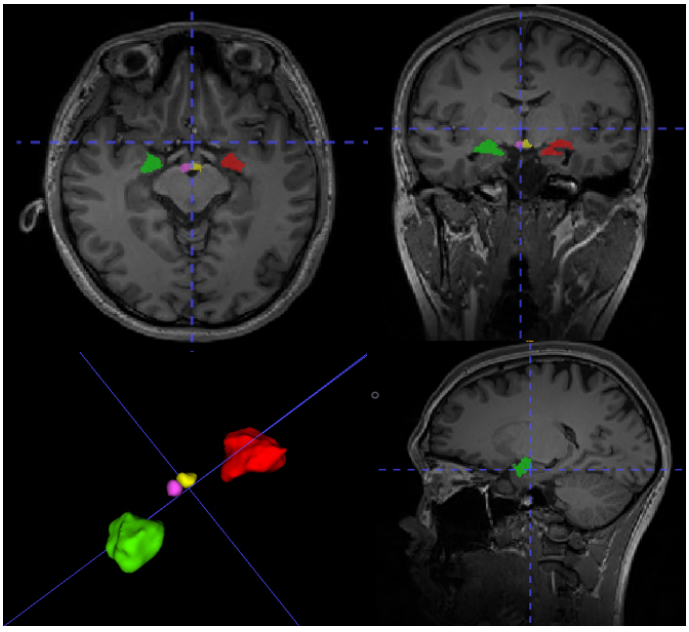


FIGURE 2. Colorization and three-dimensional modeling of MRICloud data using ITK-SNAP. Axial, coronal, and sagittal T1-weighted MR images with 3D volume renderings showing the bilateral segmentation of subcortical limbic structures using MRICloud and visualized in ITK-SNAP. Colored areas represent automatically segmented limbic structures.

Statistical Analysis

Descriptive statistics included mean, standard deviation, median, minimum, maximum, frequency, and percentage values. The distribution of variables was assessed using the Kolmogorov-Smirnov test. For the analysis of independent quantitative variables, the independent-samples t-test and the Mann-Whitney U test were used, depending on the distribution. The chi-square test was used to analyze independent categorical variables. All statistical analyses were performed using IBM SPSS Statistics version 27.0, and a significance level of $P<0.05$ was considered statistically significant.

RESULTS

The volumes of 18 subcortical brain structures were evaluated using MRICloud segmentation derived from 3D T1-weighted MRI scans. Descriptive statistics and group comparisons between patients with AD and HC are presented in Table 2.

Statistical analysis revealed that the volumes of the AmygL, AmygR, TotAmyg, HypoThL, TotHypoth, MamL, MamR, and TotMam were significantly lower in the AD group compared with the healthy control (HC) group ($P<0.05$). Additionally, the diencephalic structures - DiencL, DiencR, and TotDien - were also significantly reduced in the AD group ($P=0.001$, $P=0.012$, and $P=0.003$, respectively).

No significant volumetric differences were observed in the telencephalon (TelenL, TelenR, TotTelen), mesencephalon (Mesenc), metencephalon (Metenc), or myelencephalon (Myelenc) ($P>0.05$; Table 2). In addition to absolute volumes, inter-regional volume ratios were calculated to assess proportional relationships between adjacent brain regions. These comparisons are presented in Table 3.

The ratios of TelenL/AmygL, TelenR/AmygR,

TABLE 1. Demographic Characteristics of Alzheimer's Disease and Healthy Control Groups

Variable	Min-Max	Median (Overall)	Mean±SD (Overall)	Mean±SD (AD)	Median (AD)	Mean±SD (HC)	Median (HC)	P-value
Age (years)	55.0-84.0	70.5	70.9 ± 7.7	72.3 ± 7.7	72.5	68.9 ± 7.5	67.0	0.173[t]
Gender, n (%)								
Female			23 (58%)	14 (58%)		9 (56%)		0.896[x2]
Male			17 (43%)	10 (42%)		7 (44%)		

Data are shown as mean±standard deviation or median (minimum-maximum) or n (%). AD, alzheimer's disease; HC, healty control.

t=Independent-samples t-test, χ^2=Chi-square test

TABLE 2. Descriptive Statistics and Volumetric Comparisons of Brain Structures Between Alzheimer's Disease and Healthy Control Groups

Structure	AD group (Mean±SD)	AD group (Median)	HC group (Mean±SD)	HC group (Median)	P-value
TelenL (mm³)	438.1±47.6	444.8	454.1±43.0	466.0	0.298[t]
TelenR (mm³)	440.9±43.3	436.8	455.1±44.1	460.8	0.298[t]
TotTelen(mm³)	879.1±86.6	888.3	909.2±86.9	926.8	0.298[t]
DiencL (mm³)	6863.9±515.9	6887.5	7499.8±655.9	7428.0	**0.001[m]**
DiencR (mm³)	6965.9±578.1	6862.0	7428.9±577.3	7504.0	**0.012[m]**
TotDienc (mm³)	13.8±1.0	13.8	14.9±1.2	14.9	**0.003[t]**
Mesenc (mm³)	12.7±2.1	8.6	9.1±1.0	9.5	0.534[t]
Metenc (mm³)	141.4±21.1	136.4	136.5±21.8	131.7	0.384[t]
Myelenc (mm³)	5208.0±723.5	5364.0	5028.2±594.4	4955.0	0.414
AmygL (mm³)	1076.0±239.1	1018.0	1396.8±232.6	1322.0	**<0.001[t]**
AmygR (mm³)	1259.1±235.1	1194.0	1544.9±276.7	1528.5	**<0.001[m]**
TotAmyg(mm³)	2335.1±433.4	2211.5	2941.7±489.4	2866.5	**<0.001[m]**
HypoThL (mm³)	494.6 ± 47.3	487.0	528.4 ± 36.4	529.0	**0.020[t]**
HypoThR (mm³)	587.6±37.6	579.0	606.2±61.5	587.0	0.456[m]
TotHypoth(mm³)	1082.2±75.4	1067.0	1134.6±84.4	1131.0	**0.047[t]**
MamL (mm³)	67.9±13.2	65.0	85.2±12.5	86.0	**<0.001[t]**
MamR (mm³)	72.8±18.0	70.0	91.0±15.0	87.0	**0.002[m]**
TotMam (mm³)	140.7±28.2	135.0	176.2±24.0	176.5	**<0.001[t]**

Data are shown as mean±standard deviation or median. AD, Alzheimer's disease; HC, healty control; TelenL, left telencephalon; TelenR, right telencephalon; TotTelen, total telencephalon; DiencL, left diencephalon; DiencR, right diencephalon; TotDienc, total diencephalon; Mesenc, mesencephalon; Metenc, metencephalon; Myelenc, myelencepalon; AmygL, left amygdala; AmygR, right amygdala; TotAmyg, total amygdala; HypoThL, left hypothalamus; HypoThR, right hypothalamus; TotHypoTh, total hypothalamus; MamL, left mammillary body; MamR, right mammillary body; TotMam, total mammillary body. All volumetric data are presented in mm³, as directly obtained from MRICloud.

[t]Independent-samples t-test, [m]Mann–Whitney U test. Statistically significant P-values are shown in bold.

TABLE 3. Volume Ratios of Adjacent Brain Structures to the Amygdala, Hypothalamus, and Mammillary Body in Alzheimer's Disease and Healthy Control Groups

Ratio (Structure/Region)	AD group (Mean±SD)	AD group (Median)	HC group (Mean±SD)	HC group (Median)	P-value
TelenL/AmygL	417.3±71.9	414.5	332.4±59.2	316.3	**<0.001[m]**
TelenR/AmygR	361.0±68.0	359.4	302.7±60.1	281.5	**0.008[t]**
TelenL/HypoThL	890.3±102.6	898.7	861.5±86.2	845.8	0.360[t]
TelenR/HypoThR	751.4±70.1	750.8	756.2±94.0	744.2	0.659[m]
TelenL/MamL	6773.5±1897.0	6320.4	5415.4±788.4	5341.6	**0.009[m]**
TelenR/MamR	6425.8±1813.1	5824.1	5112.0±866.4	5046.7	**0.004[m]**
DiencL/AmygL	6.59±1.25	6.1	5.47±0.77	5.29	**0.003[t]**
DiencR/AmygR	5.71±1.04	6.1	4.94±0.88	4.84	**0.020[t]**
DiencL/HypoThL	14.0±1.9	13.9	14.2±1.9	14.0	0.662[t]
DiencR/HypoThR	11.9±1.0	11.9	12.3±1.2	11.8	0.197[t]
DiencL/MamL	105.2±23.8	103.0	89.3±13.3	84.3	**0.017[t]**
DiencR/MamR	101.7±28.1	93.2	83.5±13.7	83.3	**0.026**
Mesenc/TotAmyg	5.3±0.9	3.8	3.2±0.6	3.0	**<0.001[t]**
Mesenc/TotHypoth	11.5±1.6	8.2	8.0±0.7	7.9	0.269[t]
Mesenc/TotMam	62.9±12.9	67.2	51.6±4.3	51.6	**<0.001[t]**
Metenc/TotAmyg	62.2±13.0	63.2	47.4±10.2	45.0	**<0.001[t]**
Metenc/TotHypoth	130.9±18.9	129.4	120.7±19.5	117.5	0.106[t]
Metenc/TotMam	1047.2±296.8	954.0	783.4±131.7	769.5	**<0.001[t]**
Myelen/TotAmyg	4.83±0.9	4.60	4.45±0.6	4.19	**0.086[t]**
Myelen/TotHypoth	130.9±18.9	129.4	120.7±19.5	117.5	0.106[t]
Myelen/TotMam	140.7±28.2	135.0	176.2±24.0	176.5	**<0.001[t]**

Data are shown as mean±standard deviation or median. AD, alzheimer's disease; HC, healty control; TelenL, left telencephalon; TelenR, right telencephalon; TotTelen, total telencephalon; DiencL, left diencephalon; DiencR, right diencephalon; TotDienc, total diencephalon; Mesenc, mesencephalon; Metenc, metencephalon; Myelenc, myelencepalon; AmygL, left amygdala; AmygR, right amygdala; TotAmyg, total amygdala; HypoThL, left hypothalamus; HypoThR, right hypothalamus; TotHypoTh, total hypothalamus; MamL, left mammillary body; MamR, right mammillary body; TotMam, total mammillary body. [t]Independent-samples t-test, [m]Mann-Whitney U test. Statistically significant P-values are shown in bold.

TelenL/MamL, and TelenR/MamR; as well as DiencL/AmygL, DiencR/AmygR, DiencL/MamL, and DiencR/MamR, were all significantly higher in the AD group compared with HC (P<0.05), suggesting relatively greater volume loss in the amygdala and mammillary bodies compared with their adjacent structures. Conversely, ratios involving the hypothalamus - such as TelenL/HypoThL, TelenR/HypoThR, DiencL/HypoThL, and DiencR/HypoThR - were not statistically significant (P>0.05), indicating proportionate atrophic changes between the hypothalamus and its adjacent structures.

Moreover, when brainstem structures were evaluated relative to limbic structures, significant differences were observed in ratios such as Mesenc/TotAmyg, Mesenc/TotMam, Metenc/TotAmyg, Metenc/TotMam, and Myelenc/TotMam (P<0.001), indicating structural disproportions in these regions in the AD group (Table 3). However, the ratios of Mesenc/TotHypoth, Metenc/TotHypoth, and Myelenc/TotHypoth were not statistically significant (P>0.05), suggesting that the hypothalamus and brainstem structures undergo parallel volumetric changes in AD.

DISCUSSION

This study compared the volume ratios of selected brain structures between individuals with AD and HC. Specifically, the volume ratios of the HypoThL and TotHypoth were significantly higher in the AD group. Although the diencephalon-to-hypothalamus ratios (DiencL/HypoThL and DiencR/HypoThR) were also higher in the AD group, these differences did not reach statistical significance. This is likely because both the diencephalon (DiencL, DiencR) and the hypothalamus (HypoThL, HypoThR) exhibited similar degrees of volume reduction, resulting in comparable ratios. Moreover, the findings in Table 2 and Table 3 are consistent, as the reduction in diencephalon volume is evident both when assessed independently (Table 2) and relative to the hypothalamus (Table 3).

Recent studies emphasize that the hypothalamus plays an increasingly central role in the pathophysiology of AD, challenging earlier assumptions that primarily focused on cortical regions. Neuroimaging evidence indicates that early neurodegenerative changes may disrupt hypothalamic circuits involved in sleep, thermoregulation, and endocrine signaling - all of which are commonly impaired in AD. In particular, recent high-resolution volumetric analyses suggest that hypothalamic atrophy can occur early in the disease process, independent of global brain atrophy, making it a promising target for early diagnostic approaches [12]. This aligns with our findings, in which both absolute and ratio-based reductions in hypothalamic volume were observed in patients with AD compared with healthy controls.

Similarly, although no significant volume change was observed in the mesencephalon (Table 2), its ratio to the hypothalamus was likewise not statistically significant (Table 3). This further supports the idea that, in AD, the mesencephalon is affected to a similar extent as the hypothalamus, suggesting potential involvement of brainstem structures in disease pathology.

Adding to the existing evidence, Qu *et al*. [13] assessed the volumes of amygdala subfields using FreeSurfer software in individuals diagnosed with AD, those with mild cognitive impairment (MCI), and HC. Their results revealed significantly larger subfield volumes in the HC group compared with the AD group. Similarly, Copenhaver *et al*. [14] reported pronounced reductions in mammillary body volume in AD patients compared with individuals with MCI, other cognitive disorders, and HC.

Although mammillary bodies are integral components of the limbic circuitry, they have received relatively limited research attention over the past decade. Recent studies have begun to address this gap. For instance, Huang *et al*. [15] demonstrated that neuronal hyperactivity within the lateral mammillary nuclei may contribute to memory deficits in AD, emphasizing the region-specific vulnerability of these structures. Likewise, Salman *et al*. [16] reported heterogeneous atrophy patterns in the amygdala, with tau pathology predominantly affecting the central, medial, and accessory basal nuclei.

These findings underscore that both the amygdala and mammillary bodies are not only structurally compromised in AD but may also serve as region-specific biomarkers that reflect distinct pathological processes. Given their role in the Papez circuit, further investigation into mammillary body degeneration may offer novel insights into memory-related symptoms in Alzheimer's disease.

This study addresses this critical gap by presenting an up-to-date volumetric assessment of the mammillary bodies using an automated segmentation approach. This methodological precision enhances the reliability of volumetric measurements and contributes valuable data to an underexplored area.

In contrast to the extensive literature on hippocampal volumetry, research on other subcortical components of the limbic system has remained relatively limited. Our findings demonstrated that the volumes of the AmygL, AmygR, TotAmyg, HypoThL, TotHypoth, MamL, MamR, and TotMam were significantly lower in the AD group compared with HC.

Moreover, although the TelenL/HypoThL and TelenR/HypoThR ratios were higher in the AD group, the differences did not reach statistical significance. These findings suggest that the telencephalon undergoes volumetric changes that parallel those of the hypothalamus in AD, suggesting a broader pattern of subcortical structural degeneration associated with the disease.

Adding further context, Raji *et al*. [17] performed a volumetric comparison between bilingual and

monolingual individuals diagnosed with Alzheimer's disease (AD), examining 45 subcortical and cortical brain structures. Their findings demonstrated that monolingual individuals with AD exhibited significantly smaller volumes in the ventral diencephalon compared to their bilingual counterparts.

Consistent with these findings, our study also revealed a significant reduction in diencephalon volume when evaluated independently in AD patients compared to HC. However, when the diencephalon was analyzed relative to the hypothalamus (DiencL/HypoThL and DiencR/HypoThR), no statistically significant differences were detected between the groups. This suggests that the diencephalon undergoes atrophy parallel to that of the hypothalamus in the context of Alzheimer's disease.

By extending the current understanding of subcortical involvement, our findings provide valuable contributions to the relatively sparse literature on the role of diencephalic structures in AD pathology.

Expanding on the role of the brainstem in AD, Lee *et al*. [18] conducted an in vivo neuroimaging study that revealed significant reductions in total brainstem volume and notable structural deformities, particularly in the midbrain, in patients with AD compared to healthy individuals.

In contrast, our study did not reveal statistically significant reductions in the volumes of the mesencephalon, metencephalon, or myelencephalon when assessed individually (Table 2). Similarly, their volume ratios relative to the hypothalamus (Table 3) also showed no significant differences between groups. This pattern suggests that brainstem structures may undergo atrophy in parallel with the hypothalamus, reinforcing the hypothesis that brainstem degeneration is an integral component of AD pathology.

By combining absolute volume assessments with inter-regional ratio analyses, our study offers a refined perspective on brainstem involvement in AD, drawing attention to a structurally and functionally critical region that has been relatively underexplored in neuroimaging literature.

Strengths and Limitations

This study has several limitations that should be acknowledged. First, the relatively small sample size (24 patients with Alzheimer's disease and 16 healthy controls) may limit the generalizability of the findings. Although statistically significant differences were observed in several volumetric and ratio-based parameters, larger samples would provide greater statistical power and may reveal additional group differences not detected in this study.

Second, due to the retrospective design and reliance on previously acquired MRI scans, certain factors such as scanner variability, image quality, and acquisition protocols could not be fully standardized across all subjects. Although all images were obtained using the same 3T MRI scanner, minor technical variations may have influenced the segmentation outcomes.

Lastly, the cross-sectional nature of this study precludes conclusions about the longitudinal progression of subcortical atrophy in Alzheimer's disease. Future longitudinal studies are needed to monitor dynamic volumetric changes over time and to better evaluate the predictive value of these structural alterations as potential biomarkers.

One of the main limitations of the present study is the relatively small sample size. The data collection period coincided with the onset of the COVID-19 pandemic, and institutional safety measures implemented during this period limited researchers' access to the hospital environment, thereby restricting the number of eligible patients who could be included in the study. Nevertheless, a major strength of the present study is that it goes beyond the commonly emphasized hippocampal alterations in Alzheimer's disease and demonstrates significant volumetric changes in other components of the subcortical limbic system, particularly the amygdala, hypothalamus, and mammillary bodies. Furthermore, the combined evaluation of absolute volumetric measurements and regional volume ratios contributes to a more comprehensive characterization of proportional atrophy patterns among subcortical structures in Alzheimer's disease.

CONCLUSIONS

In conclusion, our study demonstrated significant atrophy in key subcortical limbic structures - including the bilateral amygdala, left and total hypothalamus,

and mammillary bodies - in individuals with AD. In contrast, volume ratios between diencephalic and brainstem regions and the hypothalamus showed no significant differences, suggesting a parallel pattern of atrophic change. These findings reinforce the view that AD impacts a broader subcortical network beyond the traditionally emphasized hippocampus, underscoring the importance of including these regions in future diagnostic and research frameworks.

Volumetric ratio analysis offers enhanced sensitivity in detecting inter-regional structural differences and may serve as a valuable complement to absolute volumetric assessments in future research. In this context, MRICloud stands out as a reliable and user-friendly automated platform, not only for mapping disease-associated neuroanatomical alterations but also for identifying novel subcortical biomarkers that could support early diagnosis, personalized risk stratification, and improved prognostic accuracy in clinical settings.

Ethics Approval and Consent to Participate

The study was approved by the Istanbul Medicol University Non-Interventional Clinical Research Ethics Committee (Decision no.: 170 and date: 19.02.2020). All experimental procedures involving animals were conducted in accordance with the ethical standards of the Guide for the Care and Use of Laboratory Animals published by the U.S. National Institutes of Health. All efforts were made to minimize animal suffering and to reduce the number of animals used.

Data Availability

All data generated or analyzed during this study are included in this published article. The data that support the findings of this study are available on request from the corresponding author, upon reasonable request.

Authors' Contribution

Study Conception: MED, MŞ; Study Design: MED, MŞ; Supervision: MŞ; Funding: MED, NY; Materials: MED, NY; Data Collection and/or Processing: LH, CE, GEA; Statistical Analysis and/or Data Interpretation: NY, MED; Literature Review: MED; Manuscript Preparation: MED; and Critical Review: MED.

Conflict of interest

The authors disclosed no conflict of interest during the preparation or publication of this manuscript.

Financing

This study was financially supported by the Turkish Academy of Sciences (TÜBA).

Acknowledgement

We thank TÜBA and its esteemed President, Prof. Dr. Muzaffer Şeker, for their financial and moral support.

Generative Artificial Intelligence Statement

The author(s) declare that no artificial intelligence-based tools or applications were used during the preparation process of this manuscript. The all content of the study was produced by the author(s) in accordance with scientific research methods and academic ethical principles.

Editor's note

All statements made in this article are solely those of the author(s) and do not represent the views of their affiliates or the publisher, editors, or reviewers. Any claims made by any product or manufacturer that may be evaluated in this article are not guaranteed or endorsed by the publisher.

REFERENCES

1. Livingston G, Huntley J, Liu KY, et al. Dementia prevention, intervention, and care: 2024 report of the Lancet standing Commission. Lancet. 2024;404(10452):572-628. doi: 10.1016/S0140-6736(24)01296-0.
2. Mayo Clinic. Alzheimer's disease: Symptoms and causes [Internet]. 2024 [cited 2025 Apr 3]. Available from: https://www.mayoclinic.org/diseases-conditions/alzheimers-disease/symptoms-causes/syc-20350447.
3. 2023 Alzheimer's disease facts and figures. Alzheimers Dement. 2023;19(4):1598-1695. doi: 10.1002/alz.13016.
4. Rao G, Gao H, Wang X, Zhang J, Ye M, Rao L. MRI measurements of brain hippocampus volume in relation to mild cognitive impairment and Alzheimer disease: A systematic review and meta-analysis. Medicine (Baltimore). 2023;102(36):e34997. doi: 10.1097/MD.0000000000034997.
5. Scarmeas N, Hadjigeorgiou GM, Papadimitriou A, et al. Motor signs during the course of Alzheimer disease. Neurology. 2004;63(6):975-982. doi: 10.1212/01.wnl.0000138440.39918.0c.
6. Mega MS, Lee L, Dinov ID, Mishkin F, Toga AW, Cummings JL. Cerebral correlates of psychotic symptoms in Alzheimer's

disease. J Neurol Neurosurg Psychiatry. 2000;69(2):167-171. doi: 10.1136/jnnp.69.2.167.
7. Braak H, Braak E. Alzheimer's disease affects limbic nuclei of the thalamus. Acta Neuropathol. 1991;81(3):261-268. doi: 10.1007/BF00305867.
8. Forno G, Lladó A, Hornberger M. Going round in circles-The Papez circuit in Alzheimer's disease. Eur J Neurosci. 2021;54(10):7668-7687. doi: 10.1111/ejn.15494.
9. Gerritsen L, Rijpkema M, van Oostrom I, et al. Amygdala to hippocampal volume ratio is associated with negative memory bias in healthy subjects. Psychol Med. 2012;42(2):335-343. doi: 10.1017/S003329171100122X.
10. Sakamoto R, Marano C, Miller MI, et al. Cloud-Based Brain Magnetic Resonance Image Segmentation and Parcellation System for Individualized Prediction of Cognitive Worsening. J Healthc Eng. 2019;2019:9507193. doi: 10.1155/2019/9507193.
11. Hannoun S, Tutunji R, El Homsi M, Saaybi S, Hourani R. Automatic Thalamus Segmentation on Unenhanced 3D T1 Weighted Images: Comparison of Publicly Available Segmentation Methods in a Pediatric Population. Neuroinformatics. 2019;17(3):443-450. doi: 10.1007/s12021-018-9408-7.
12. Xu P, Estrada S, Etteldorf R, et al. Hypothalamic volume is associated with age, sex and cognitive function across lifespan: a comparative analysis of two large population-based cohort studies. EBioMedicine. 2025;111:105513. doi: 10.1016/j.ebiom.2024.105513.
13. Qu H, Ge H, Wang L, Wang W, Hu C. Volume changes of hippocampal and amygdala subfields in patients with mild cognitive impairment and Alzheimer's disease. Acta Neurol Belg. 2023;123(4):1381-1393. doi: 10.1007/s13760-023-02235-9.
14. Copenhaver BR, Rabin LA, Saykin AJ, et al. The fornix and mammillary bodies in older adults with Alzheimer's disease, mild cognitive impairment, and cognitive complaints: a volumetric MRI study. Psychiatry Res. 2006;147(2-3):93-103. doi: 10.1016/j.pscychresns.2006.01.015.
15. Huang WC, Peng Z, Murdock MH, et al. Lateral mammillary body neurons in mouse brain are disproportionately vulnerable in Alzheimer's disease. Sci Transl Med. 2023;15(692):eabq1019. doi: 10.1126/scitranslmed.abq1019.
16. Salman Y, Gérard T, Huyghe L, et al; Alzheimer's Disease Neuroimaging Initiative. Amygdala atrophies in specific subnuclei in preclinical Alzheimer's disease. Alzheimers Dement. 2024;20(10):7205-7219. doi: 10.1002/alz.14235.
17. Raji CA, Meysami S, Merrill DA, Porter VR, Mendez MF. Brain structure in bilingual compared to monolingual individuals with Alzheimer's disease: Proof of concept. J Alzheimers Dis. 2020;76(1):275-280. doi: 10.3233/JAD-200200.
18. Lee JH, Ryan J, Andreescu C, Aizenstein H, Lim HK. Brainstem morphological changes in Alzheimer's disease. Neuroreport. 2015;26(7):411-415. doi: 10.1097/WNR.0000000000000362.